

Biose, I. J., Dewar, D., Macrae, I. M. and McCabe, C. (2019) Impact of stroke co-morbidities on cortical collateral flow following ischaemic stroke. *Journal of Cerebral Blood Flow and Metabolism*, (doi:[10.1177/0271678X19858532](https://doi.org/10.1177/0271678X19858532)).

This is the author's final accepted version.

There may be differences between this version and the published version. You are advised to consult the publisher's version if you wish to cite from it.

<http://eprints.gla.ac.uk/187676/>

Deposited on: 14 June 2019

FULL TITLE: Impact of stroke co-morbidities on cortical collateral flow following ischaemic stroke

Ifechukwude Joachim Biose MSc ^{1,2}, Deborah Dewar PhD¹, I. Mhairi Macrae PhD ¹ and Christopher McCabe PhD¹.

1. Stroke and Brain Imaging, Institute of Neuroscience and Psychology, College of Medical, Veterinary and Life Sciences, University of Glasgow, United Kingdom.

2. Department of Anatomy and Forensic Anthropology, Cross River University of Technology, Nigeria.

Corresponding Author:

Ifechukwude Joachim Biose,

Email: i.biose.1@research.gla.ac.uk, ifybio@gmail.com

Phone: +18594943446

Sources of funding: Tertiary Education Trust Fund & the University of Glasgow.

Running Headline: Stroke comorbidities on cortical collateral flow

ABSTRACT

Acute hyperglycaemia and chronic hypertension worsen stroke outcome but their impact on collateral perfusion, a determinant of penumbral life span, is poorly understood. Laser-speckle contrast imaging (LSCI) was used to determine the influence of these stroke comorbidities on cortical perfusion after permanent middle cerebral artery occlusion (pMCAO) in Spontaneously Hypertensive Stroke Prone rats (SHRSP) and normotensive Wistar rats. Four independent studies were conducted. In animals without pMCAO, cortical perfusion remained stable over 180 minutes. Following pMCAO, cortical perfusion was markedly reduced at 30 minutes then gradually increased, via cortical collaterals, over the subsequent 3.5 hours. In the contralateral non-ischaemic hemisphere perfusion did not change over time. Acute hyperglycaemia (in normotensive Wistar) and chronic hypertension (SHRSP) attenuated the restoration of cortical perfusion after pMCAO. Inhaled nitric oxide did not influence cortical perfusion in SHRSP following pMCAO. Thus, hyperglycaemia at the time of arterial occlusion or pre-existing hypertension impaired the dynamic recruitment of cortical collaterals after pMCAO. The impairment of collateral recruitment may contribute to the detrimental effects these comorbidities have on stroke outcome.

Keywords: Acute hyperglycaemia, cortical collateral perfusion, hypertension, ischaemic stroke, laser speckle contrast imaging.

INTRODUCTION

Stroke is a leading cause of permanent disability and accounts for approximately 12% of all deaths in the world each year.¹ Ischaemic stroke, caused by an occlusion of a cerebral blood vessel, represents 85% of all cases.² The established treatments for ischaemic stroke are recanalisation of the occluded artery in order to allow reperfusion of the downstream territory: thrombolysis with recombinant tissue plasminogen activator (r-tPA) or endovascular thrombectomy.^{3,4,5,6,7} However, only a small proportion of stroke patients are eligible for these therapies due to a narrow therapeutic time window (<4.5 h for rt-PA & <6 h for thrombectomy) and risk of bleeding.⁸

Following ischaemic stroke, the cerebral collateral circulation, a network of anastomoses between cerebral arteries, helps to maintain cerebral blood flow (CBF).^{9,10} Leptomeningeal anastomoses (LMAs) are a network of pial arterioles that make connections between the middle, anterior and posterior cerebral arteries. They provide a means of blood flow recruitment to the cortical layers of an occluded arterial territory.¹¹ These blood vessels dilate in response to a variety of direct neural, metabolic and haemodynamic factors.¹² However, the primary factor that determines the direction of flow is the fall in hydrodynamic pressure at the distal ends of the affected major arteries. Effective collateral blood flow recruitment is known to extend the survival time of the injured, hypoperfused and potentially salvageable ischaemic penumbra as well as improve outcome following recanalisation therapies.^{12,13,14} Likewise, preclinical

evidence suggests that the quantity and dimension of LMAs is inversely related to neuronal death following stroke.¹⁵ The extent of collateral flow may explain the considerable number of patients that maintain a small ischaemic core and a significant penumbra beyond six hours and for up to several days following symptom onset^{16,17} while other patients have aggravated brain tissue death and enlarged ischaemic core.^{17,18,19,20}

Established stroke co-morbidities (i.e. hypertension & acute hyperglycaemia) are associated with worse outcome following stroke.^{21,22,23} There is a paucity of information on the impact of stroke co-morbidities on the dynamics of cortical collateral recruitment during the first hours post-stroke. Understanding the dynamics of collateral recruitment to support the ischaemic penumbra until CBF through the occluded artery is restored, may drive the development of new adjunct therapies. Hence, to study the evolution of collateral perfusion after ischaemic stroke we used a rat permanent middle cerebral artery occlusion (pMCAO) model, and Laser speckle contrast imaging (LSCI), which combines high temporal and spatial resolution, to quantify relative CBF²⁴.

The principal aims were to characterise the dynamic changes in cortical collateral perfusion during the first critical hours following pMCAO, the influence of known stroke risk factors (acute hyperglycaemia and hypertension) and the impact of a potential therapeutic, inhaled nitric oxide (iNO) to enhance the recruitment of collateral perfusion.

METHODS

Animals and study groups

- A. A total of sixty-five male rats (Wistar, n=38 and spontaneously hypertensive stroke-prone rat (SHRSP), n=27; 300-365 g) were randomly allocated to study and treatment groups according to specific aims, using random.org in four separate studies: A. To determine the dynamic changes in cortical perfusion following stroke (Wistar rats): Control (n=6) and pMCAO (n=10).
- B. To determine the influence of acute hyperglycaemia on cortical perfusion: pMCAO+vehicle (Wistar, n=11) and pMCAO+glucose (Wistar, n=11).
- C. To characterise the impact of chronic hypertension on the dynamic recruitment of collateral perfusion in SHRSP (pMCAO, n=9).
- D. To determine if iNO enhances the recruitment of cortical collateral perfusion in the presence of chronic hypertension: pMCAO+Air (SHRSP, n=9) and pMCAO+iNO (SHRSP, n=9).

Wistar rats were purchased from Charles River and the SHRSPs were bred in a colony maintained at the Institute of Cardiovascular and Medical Sciences, University of Glasgow. All rats were maintained in identical housing conditions: strain and age-matched groups of four rats per cage, standard 12 h light-dark cycle along with unlimited access to water and chow. A minimum of one week from date of delivery

was allowed for acclimatisation. For study B (hyperglycaemia), rats were restricted to two chow pellets overnight for 15-17 h prior to experimentation. This was to ensure baseline normoglycaemia (blood glucose concentration of 2.6-5.3 mmol/L in rats.²⁵) under general anaesthesia. All animal procedures were approved by the University of Glasgow Ethical Review Panel and performed under the UK Home Office Project Licences, 60/4449 and P643E89D8 for Preclinical Stroke and Experimental MRI and subject to the Animals (Scientific Procedures) Act of 1986 incorporating European Directive 2010/63/EU. Experiments were carried out according to ARRIVE guidelines (<http://www.nc3rs.org.uk/arrive-guidelines>) during planning, experimentation, analysis and documentation of all procedures.

Anaesthesia

Using aseptic surgical technique, anaesthesia was induced (5% isoflurane) and, following oral intubation, maintained (2-3% isoflurane) during surgical preparation with artificial ventilation in a mixture of air:oxygen (1 L/min air, 0.2 L/min O₂). To reduce tracheal secretions and pain, atropine sulphate (0.05 mg/kg, s.c.) and ropivacaine hydrochloride (Norapin[®]; 0.2 ml s.c.) were administered over the abdomen and calvaria (site of cranial incision), respectively. Following completion of surgical procedures, isoflurane was reduced to 1% and then gradually turned off during a bolus (80 mg/kg i.v.) and then continuous infusion (30 mg/kg/hr i.v.) of alpha-chloralose

(AC) for imaging and to maintain cerebral autoregulation and neurovascular coupling. Body temperature was maintained at 37 ± 0.5 °C and blood pressure, arterial blood gases (PaO_2 , PaCO_2), blood pH and glucose were monitored throughout the experimental protocol.

Middle cerebral artery occlusion & imaging window

Rats were placed in a stereotaxic frame for skull thinning prior to induction of MCAO. The entire cortical surface was thinned using a dental drill, ensuring that the dura was left intact. Rats were removed from the stereotaxic frame for induction of pMCAO which employed a minor modification of the intraluminal filament model of Koizumi et al.²⁶ Briefly, permanent ligatures (4-0 sutures) were placed at the proximal portion of the CCA, external carotid, occipital and pterygopalatine arteries. A 4-0 nylon silicone coated tip monofilament (404134PK10 and 50-3033PKRe for Wistar and SHRSP rats; Doccol Corporation, MA, USA) was inserted into the CCA and gently advanced until resistance was felt, indicating occlusion at the origin of the middle cerebral artery (MCA). The non-stroke control group received similar anaesthetic treatments for equivalent duration as well as calvaria thinning.

Induction of acute hyperglycaemia

Rats were randomly allocated to receive either vehicle (saline) or glucose (15%; 10 ml/kg) administered i.p. 10min prior to pMCAO, as previously described.²³ Blood glucose levels were measured at baseline and at multiple time points following pMCAO using a glucometer (Accu-Check).

Laser speckle contrast imaging (LSCI) and analysis

Following the induction of pMCAO, rats were returned to the stereotaxic frame with their heads secured by tooth and ear bars to avoid movement artefact while imaging. Paraffin oil (JOHNSON'S® baby oil, USA) was applied to the surface of the thinned skull to ensure a stable signal during imaging. Real time changes in cortical blood flow were recorded by means of a Laser speckle contrast imager (PeriCam PSI HD system, Perimed, Stockholm, Sweden), acquired from the estimation of intravascular red blood cell movement from a stack of images following 6 ms exposure time and programmed to produce 9 pixels (3x3) for contrast calculation.

Perfusion values are calculated as $((1/C) - 1)$, where C is the contrast. The penetration depth of the laser (785 nm) is approximately 500 μm below the thinned skull ensuring imaging of the cortical vessels on the brain surface. Temporal resolution was set at an effective frame rate of 0.2 images/second (averaging 5 images) with a spatial resolution of 20 μm . A minimum stabilisation period of 10min was allowed under the laser

speckle contrast imager, before baseline recording commenced at 30 min from the onset of stroke, and continued until 4h post-MCAO.

Cortical blood flow data for each rat were processed and extracted using PIMSoft (Perimed, Stockholm, Sweden). Regions of interest (ROIs) were established at 30min post-MCAO (baseline) based on the following blood flow thresholds:^{27,28,29} ischaemic core (<43% of mean contralateral hemisphere); hypoperfused tissue (CBF between 43-75% of mean contralateral hemisphere) along with contralateral equivalent ROIs as shown in Figure 1C. For the control group, the entire ipsilateral and contralateral hemispheres were taken as the ROIs. Blood flow data from each ROI were normalised to the respective mean blood flow during the first 10min at baseline (30 min post-MCAO).

Delivery of inhaled nitric oxide

To determine if iNO can increase collateral flow in SHRSP, rats were randomised to receive either Air or iNO (60 ppm) starting at 30 min post-MCAO. Nitric oxide (NO) gas was delivered in the ventilatory gas mixture and the concentrations of NO₂ and O₂ were monitored and controlled using the INOMAX monitoring system (USA). NO₂ concentration was maintained below 1.2 ppm, a level assumed to be toxic to the lungs,³⁰ for the duration of the experiments.

Blinding and statistical analysis

The experimenter was blind to group identity during data analysis for studies A, B and D as well as group identity during surgery & induction of hyperglycaemia for study B. All data were analysed using Graphpad Prism 6 (GraphPad Software, USA) and are presented as mean \pm SD. Mean normalised blood flow and mean arterial blood pressure (MABP) data were collected every 10min for statistical analysis. To determine differences in blood flow within tissue compartments, area under curve for each ROI was calculated. Unpaired Student's t-test, multiple comparison 1-way ANOVA followed by Dunett's test or repeated measures 2-way ANOVA followed by Sidak's test were used to test the statistical significance of differences between groups, set at $p<0.05$.

RESULTS

Dynamic recruitment of cortical perfusion following pMCAO

Real time changes in cortical perfusion during the first hours following pMCAO were assessed in normotensive Wistar rats and compared with control non-stroke Wistar rats. Physiological variables were stable throughout the experimental protocol with no significant differences between groups ($F(2,28)=0.1049$, $p=0.9008$ for pH, $F=0.08536$, $p=0.9184$ for PaO_2 , $F=2.123$, $p=0.1385$ for PaCO_2 and $F=1.881$, $p=0.1712$ for body temperature. Supplemental Table 1).

Cortical perfusion within the ischaemic core in the pMCAO group increased by $215\pm131\%$ by 2.5h post-MCAO when compared to baseline (30 min pMCAO, Figure 2B). Cortical perfusion within the hypoperfused ROI also increased over the time course ($170\pm97\%$). This increase in perfusion within the ischaemic core and hypoperfused regions was significantly different compared to perfusion data for the equivalent contralateral ROIs ($F(2,23)=5.763$, $p=0.0094$; Figure 2C). No significant increase in cortical perfusion was observed within these ROIs ($19\pm5\%$ for ischaemic core and $19\pm7\%$ for hypoperfused ROIs, respectively, $F(2,23)=1.439$, $p=0.2578$, Figure 2D and 2E) indicating that this increase in blood flow is specific to the ischaemic hemisphere. Importantly, no significant change ($F(13,182)=0.8987$, $p=0.5556$) in mean arterial blood pressure (MABP) was observed over the duration of

the experimental protocol indicating that the increase in blood flow was not driven by changes in systemic blood pressure (Figure 2F). The increase in ipsilateral cortical blood flow originated from the midline, at the boundary of the initial blood flow deficit, moving towards the ischaemic core. This suggests the recruitment of cortical collateral vessels (leptomeningeal anastomoses) rather than an increase in flow through the occluded MCA (see 2nd row of Figure 2A). In control non-stroke rats, there was no change in blood flow over the same time course (1st row of Figure 2A).

Impact of acute post-stroke hyperglycaemia on cortical perfusion

Real time changes in cortical perfusion were assessed in a model of acute hyperglycaemia following pMCAO in normotensive rats and vehicle-treated control rats. Physiological variables were within reference ranges throughout the experimental protocol with no significant differences between groups ($F(4,80)=1.642$, $p=0.1279$ for pH, $F=0.5482$, $p=0.7009$ for PaO_2 , $F=1.077$, $p=0.3887$ for PaCO_2 and $F=1.054$, $p=0.346$ for body temperature, Supplemental Table 2). Blood glucose concentration was significantly higher ($F(5,120)=20.28$, $p=0.0001$) at all time points with peak values at 30min post-MCAO for pMCAO+glucose rats when compared to pMCAO+vehicle group (Figure 3K). This confirmed successful induction and maintenance of a clinically relevant level of acute hyperglycaemia.

Cortical perfusion within the ischaemic core increased by $212\pm 80\%$ and $78\pm 11\%$ in the pMCAO+vehicle and pMCAO+glucose groups, respectively, by 4h post-MCAO when compared to baseline (Figure 3B). The increase in cortical perfusion within the ischaemic core of normoglycaemic rats was significantly attenuated in the presence of hyperglycaemia (t , $df=2.530, 11$, $p=0.0280$, Figure 3C). A similar increase in cortical perfusion was observed over the time course in the hypoperfused ROI in the pMCAO+vehicle group ($156\pm 71\%$) and this increase was attenuated in the pMCAO+glucose treated rats ($82\pm 10\%$, Figure 3D). The difference between groups did not achieve statistical significance ($t, df=1.468, 18$, $p=0.1593$, Figure 3E). In the contralateral hemisphere there was a small change in cortical perfusion within the homotopic contralateral ischaemic core ROI over the time course in both groups (change in perfusion: contralateral to ischaemic core, $35\pm 43\%$ vs $3\pm 7\%$ for vehicle and glucose groups, respectively, Figure 3F). A similar change in cortical perfusion was observed within the homotopic contralateral hypoperfused ROI (change in perfusion: $30\pm 58\%$ vs $5\pm 6\%$ for vehicle and glucose groups, respectively, Figure 3H). Within the contralateral hemisphere the small increase in perfusion in both ROIs in the normoglycaemic group was significantly attenuated in the hyperglycaemic group ($t, df=2.975, 11$, $p=0.0126$ and $t, df=2.324, 18$, $p=0.0320$, respectively, Figure 3G and 3I). No significant change ($F(17,360)=0.9064$, $p=0.5667$) in MABP was observed over the duration of the experimental protocol (Figure 3J), indicating that blood pressure did not

influence the impaired recruitment of cortical collateral blood vessels in the pMCAO+glucose group when compared to pMCAO+vehicle (Figure 3A).

Impact of chronic hypertension on cortical perfusion following pMCAO

Physiological variables in SHRSP were within reference ranges throughout the experimental protocol (Supplemental Table 3). There was no significant change in cortical perfusion within the ipsilateral hemisphere of SHRSPs throughout the time course (change in perfusion from baseline to 4h: $5\pm 23\%$ & $5\pm 19\%$ for the ischaemic core and hypoperfused ROIs, respectively; Figure 4B and 4D). Similarly, there was no change in cortical perfusion throughout the time course in the contralateral ROIs (change in perfusion from baseline to 4h: $10\pm 10\%$ and $10\pm 9\%$ for the contralateral ischaemic core and hypoperfused ROIs, respectively; Figure 4B and 4D). The recruitment of cortical collateral blood vessels was impaired (Figure 4A) despite stable MABP observed throughout the experimental protocol (Figure 4F).

Investigation of the potential of intervention to enhance blood flow following pMCAO

The effect of iNO (at 60ppm) on cortical perfusion was measured following pMCAO in SHRSP and compared to control SHRSP that received air only. Figure 5A shows an example perfusion map from the median animal from each group over time.

Physiological variables were within reference ranges throughout the experimental protocol with no significant differences between groups ($F(3,48)=0.8152$, $p=0.4978$ for pH, $F=0.4128$, $p=0.7410$ for PaO_2 , $F=0.2249$, $p=0.8786$ for PaCO_2 and $F=1.127$, $p=0.3474$ for body temperature. Supplemental Table 4). For both groups, arterial blood glucose concentration was slightly raised ($>6\text{mmol/L}$) 10min prior to the induction of pMCAO but returned to the normal range ($3.5\leq 6\text{mmol/L}$) from 1h post-MCAO until the end of experimental protocol (see Figure 5K). No significant differences were observed between groups throughout the protocol.

There was no significant difference in cortical perfusion between iNO and vehicle-treated rats in the ischaemic core (change in perfusion from baseline to 4hr pMCAO: $16\pm 14\%$ vs $8\pm 1\%$ for air & iNO groups, respectively) and hypoperfused ROIs ($10\pm 20\%$ vs $4\pm 2\%$ for air & iNO groups, respectively. Figure 5B & D). Area under the curve analysis confirmed that there were no differences in cortical perfusion over time and between treatment groups (Figure 5C & E). Within the contralateral equivalent ROIs there was no change in cortical perfusion over time and between treatment groups (Figures 5G& I).

Stable MABP was observed over the duration of the experimental protocol with no significant difference between groups ($F(20, 320)=0.5966$, $p=0.9146$, Figure 5J), indicating that iNO did not alter MABP.

DISCUSSION

The present study demonstrates, for the first time, the dynamic recruitment of cortical collateral perfusion during the first critical hours following experimental stroke in rat models with and without known stroke risk factors. LSCI revealed stable, cortical flow over the duration of imaging (4h) in non-stroke control Wistar rats. Following cortical ischaemia induced by pMCAO, cortical collateral perfusion gradually increases within the ischaemic hemisphere. In contrast, the presence of clinically relevant levels of acute post-stroke hyperglycaemia results in a significant attenuation in the recruitment of cortical collateral perfusion. Similarly, rats with chronic hypertension (SHRSP) demonstrate a failure of cortical collateral perfusion recruitment after pMCAO. Finally, we found that iNO did not ameliorate the failed recruitment of cortical collateral perfusion demonstrated in SHRSP following pMCAO.

LSCI acquires perfusion data from the estimation of intravascular red blood cell movement from a stack of images²⁴. LSCI therefore provides real time full-field imaging with robust temporal and spatial resolution suitable for the dynamic quantification of blood flow in the vasculature of the cortex. The benefits of LSCI include a relatively faster signal processing time and near real-time blood flow estimates for the semi-invasive investigation of blood flow dynamics with excellent

reproducibility when compared to other optical and non-optical imaging systems.^{31,32,33,24} However, LSCI also presents some limitations which include: distortion of the overall estimates by static artefacts⁷⁶ as well as shallow penetration of the laser rays which requires the surgical removal or thinning of the calvaria for rat cerebral studies.²⁴ Also, LSCI data cannot be used to directly compare between animals or timepoints without data normalisation. This is because LSCI does not provide absolute perfusion values owing to the undefined mathematical relationship between speckle contrast and blood flow velocity.^{71,72}

Regarding collateral perfusion following stroke, increased cortical perfusion was detected in the ipsilateral ischaemic core and hypoperfused ROIs during the first 3-4 hours following pMCAO in two separate groups of rats (normotensive and normoglycaemic animals in studies A & B) and importantly, was specific to the ischaemic hemisphere since no significant changes in perfusion were observed within the contralateral hemisphere of these animals or in non-stroke control rats. The increased perfusion in the ischaemic territory is likely to reflect the recruitment of collateral vessels lying close to the midline, and adjacent to the cerebral region known to be supplied by the anterior cerebral artery (ACA) in rats. The increase in collateral perfusion following pMCAO is a compensatory mechanism to redirect blood supply to the ischaemic region in order to maintain blood flow and potentially salvage the

ischaemic penumbra.³³ These observations support and extend earlier studies of collateral flow. Ten minutes following pMCAO, Strong et al.³⁴ reported an approximate 50-70% increase in CBF in the core and hypoperfused regions of the gyrencephalic cortex in cats. The blood flow recovery was near pre-occlusion values by 90min post-MCAO. Similarly, a variable recruitment of collateral perfusion has been reported in normotensive and normoglycaemic rats where anastomotic connections between ACA and MCA were observed following the induction of MCAO. In an embolic MCAO model in Sprague-Dawley rats, Armitage et al.³⁵ reported an immediate anastomotic connection established between the branches of ACA and MCA which persisted for up to 24h. In a different study, these anastomotic connections following pMCAO in Sprague-Dawley rats were classified into three categories, viz: transient, impermanent and persistent, based on their dynamic evolution 3h following recruitment.³⁶ Also, cortical vessel recruitment following ischaemic stroke has been reported in humans.^{37,38}

Changes in vascular physiology (MABP, blood pH, PaO₂ and PaCO₂) due to anaesthesia may potentially impact on cerebral blood flow. Hence, all rats were mechanically ventilated to prevent respiratory depression and AC anaesthesia chosen for the LSCI session to limit anaesthesia effects on vascular physiology and cerebral blood flow.^{39,40} PaCO₂ in particular is known to dilate cerebral vessels and increase

CBF.^{41,42} Therefore, for all study groups and treatments, blood physiological parameters (PaCO₂, PaO₂, and pH) and body temperature were monitored and maintained within the normal range. Small differences in MABP between groups were not statistically significant. Therefore, differences in physiological parameters were not responsible for the observed changes in the recruitment of collateral perfusion following pMCAO.

The physiological recruitment of collaterals following pMCAO was impaired in our rat model of acute hyperglycaemia. This may explain, in part at least, our previous report of more rapid growth of ischaemic brain lesions, as determined by diffusion-weighted MRI, following pMCAO in acute hyperglycaemic rats compared to normoglycaemic controls.²³ It is also consistent with patient studies linking acute hyperglycaemia (defined as sustained blood glucose concentration above 6.0 mmol/L), with poorer functional outcome and higher mortality following stroke.^{47,48,49,50,51,52,53,54} Further, a recent study⁵⁵ showed that hyperglycaemia in stroke patients with good collaterals decreases clinical prognosis and had no effect on patients with poor collateral recruitment. This suggests that high blood glucose around the time of stroke is detrimental to neurological recovery in stroke patients with otherwise functional collateral capacity.

In a recent rat study, our group assessed the influence of acute hyperglycaemia on cerebral blood flow after pMCAO using alternative CBF methods. Using in vivo autoradiography and perfusion-weighted MRI there was no detectable effect of this level of hyperglycaemia on CBF, although ischaemic brain damage was increased.⁵⁶ These seemingly contradictory findings may reflect the different sensitivities of autoradiography and MRI versus LSCI with the latter providing a more sensitive method of assessing changes in cerebral perfusion. The pathophysiological mechanism for the impaired recruitment of collateral flow in acute post-stroke hyperglycaemia is not yet clear. However, raised blood glucose concentration is known to inhibit NO-mediated vasodilatation, partly due to an induced decrease in NO bioavailability.^{57,58} Another important factor that has been suggested is hyperglycaemia-induced blood coagulation and fibrinolysis dysfunction leading to increased blood viscosity and impaired erythrocyte functions.⁵⁹

Hypertension is an important risk factor for stroke which also worsens functional outcome in humans.^{60,61} Owing to the spontaneous development of essential hypertension (~220mmHg systolic) and stroke, SHRSPs represent one of the most clinically relevant rat models of chronic hypertension in pre-clinical research.^{62,63} The genetically related spontaneously hypertensive rat (SHR, ~180mmHg systolic), which rarely shows signs of spontaneous stroke, is also widely used^{64,65}.

Our observation of the impaired recruitment of collateral flow in the SHRSP is consistent with a previous report.⁶⁶ Coyle and Heistad⁶⁶ quantified the anastomoses between the ACA and MCA in the normotensive control Wistar Kyoto strain (WKY) and SHRSP. They showed no reduction in the number of anastomoses but a considerable narrowing of the collateral anastomoses in SHRSP compared to WKY and following MCAO. When compared to WKY, we and others have also reported an increased sensitivity of SHRSP to stroke^{67,68,69} as well as the rapid infarction of the penumbral tissue apparent within 1h following pMCAO.^{21,22} Hypertension is associated with vasoconstriction in cerebral vessels and decreased vasorelaxation. The *ex vivo* study of Chan et al.⁷⁰ showed luminal constriction of LMAs isolated from young (18 weeks old) and aged (48 weeks old) SHR when compared to normotensive WKYs. Also, the study reported that small intraluminal pressure stimulation of 20 mmHg resulted in more constriction of LMAs from young SHR when compared with aged SHRs. Recently, using multisite laser doppler flowmetry, further studies from the same group^{64,65} reported poor collateral perfusion during 2 h transient MCAO in aged and young SHRs. These findings of collateral failure in SHR are in agreement with the results of the present studies in SHRSP and provide evidence for beneficial effects of oxygen-based therapy and PAI-1 inhibition on collateral function.⁷¹

Increased glutamate concentration,⁷² and the increased levels of the powerful vasoconstrictor, 20-HETE, in the brain of SHRSPs following ischaemic stroke⁷³ may also contribute to the impairment of cortical collateral flow. Dunn et al.⁷³ showed that the suppression of 20-HETE with intracerebral injection of HET-0016, a potent inhibitor of 20-HETE, reduced infarct volume following stroke. However, iNO at 60ppm, a potent vasodilator shown to selectively dilate cerebral blood vessels in the ischaemic territory of normotensive mice,⁷⁴ did not ameliorate the impaired recruitment of collateral perfusion in the SHRSP, in our hands, following pMCAO.

Taken together the data reported here demonstrate that hypertension or acute post-stroke hyperglycaemia impair the recruitment of collateral perfusion following ischaemic stroke in rats. These findings provide insight into the rapid evolution of brain damage and decreased volume of salvageable brain tissue, as well as the aggravated outcome following stroke in the presence of these comorbidities, and provide an experimental platform to test therapies designed to support penumbra until reperfusion is induced. In addition to age, hyperuricaemia and metabolic syndrome have also been associated with poor collateral status in human stroke patients.⁵⁴ Hence, in the continuous quest for effective collateral flow enhancers, these stroke comorbidities should also be considered. This study is subject to some limitations. Firstly, we did not carry out statistical power calculation *a priori* to determine group

size. Secondly, we did not include a normotensive strain for our SHRSP group in study C, and lastly, we did not assess infarct or lesion volume. The paper presents an exploratory insight to the potential of LSCI to study collateral recruitment and how the contributors of worsened stroke outcome (chronic hypertension and acute hyperglycaemia) influence the recruitment of collateral perfusion following stroke. UK animal regulation does not permit recovery of animals under prolonged AC anaesthesia.

In conclusion, we present novel longitudinal *in vivo* data demonstrating significantly attenuated cortical collateral perfusion in the presence of known risk factors such as acute post-stroke hyperglycaemia and chronic hypertension. This impaired recruitment of collateral perfusion may in part explain the worse outcome and accelerated growth of brain damage in the presence of these risk factors. In addition, we have shown that inhaled NO does not enhance collateral perfusion following stroke in a rat model with pre-existing hypertension. In agreement with previous reports^{75,76,77} we show that LSCI is an effective tool to investigate cortical blood flow changes following pre-clinical treatments or experimental manipulations *in vivo*. In combination with animal models of stroke comorbidities LSCI promises to be a robust tool in the development of vasodilators or cerebral blood flow enhancers and the evaluation of their real time

cerebrovascular effects in the setting of preclinical stroke and other neurovascular applications.

ACKNOWLEDGEMENTS: This study was funded by Tertiary Education Trust Fund & the University of Glasgow.

AUTHOUR CONTRIBUTION STATEMENT: All authors contributed to the concept/design of the experiments, article revision and approval for publication. **Biose IJ** conducted all experiments, analysed and interpreted all data as well as wrote the draft. **Dewar D** conceived and designed the acute hyperglycaemia experiments and revised the draft. **Macrae IM** and **Mccabe C** jointly conceived, designed and supervised all other experiments as well as revised the draft.

DISCLOSURES/CONFLICT OF INTEREST: None

Supplementary material for this paper can be found at <http://jcbfm.sagepub.com/content/by/supplemental-data>

REFERENCES

1. Feigin VL, Norrving B, Mensah GA. Global burden of stroke. *Circ Res* 2017; 120: 439-448.
2. Intercollegiate Stroke Working Party. National clinical guideline for stroke. 5th Edition. London: Royal College of Physicians. 2016.
3. Berkhemer OA, Fransen PS, Beumer D et al. A randomized trial of intraarterial treatment for acute ischemic stroke. *Engl J Med* 2015; 372(1): 11-20.
4. Goyal M, Demchuk AM, Menon BK et al. Randomized assessment of rapid endovascular treatment of ischemic stroke. *N Engl J Med* 2015; 372: 1019.
5. Campbell BC, Mitchell PJ, Kleinig TJ et al. Endovascular therapy for ischemic stroke with blood flow-imaging selection. *N Engl J Med* 2015; 372: 1009.
6. Saver JL, Goyal M, Bonafe A et al. Stent-retriever thrombectomy after intravenous t-PA vs. t-PA alone in stroke. *N Engl J Med* 2015; 372: 2285.
7. Jovin TG, Chamorro A, Cobo E et al. Thrombectomy within 8 hours after symptom onset in ischemic stroke. *N Engl J Med* 2015; 372: 2296.
8. Chia NH, Leyden JM, Newbury J et al. Determining the Number of Ischemic Strokes Potentially Eligible for Endovascular Thrombectomy: A Population-Based Study. *Stroke* 2016; 47: 1377.
9. Brozici M, Zwan A, Hillen B. Anatomy and Functionality of Leptomeningeal Anastomoses (A Review). *Stroke* 2003; 34: 2750-2762.

10. Sheth SA, Liebeskind DS. Imaging evaluation of collaterals in the brain: physiology and clinical translation. *Curr Radiol Rep* 2014; 2(1): 29.
11. Shuaib A, Butcher K, Mohammad AA et al. Collateral blood vessels in acute ischaemic stroke: a potential therapeutic target. *Lancet Neurol* 2011A; 10: 909–921.
12. Liebeskind DS. Collateral circulation. *Stroke* 2003; 34: 2279–84.
13. Shuaib A, Bornstein NM, Diener HC et al. Partial aortic occlusion for cerebral blood flow augmentation: safety and efficacy of NeuroFlo in Acute Ischemic Stroke trial. *Stroke* 2011B; 42: 1680–90.
14. Liu J, Wang Y, Akamatsu Y et al. Vascular remodeling after ischemic stroke: mechanisms and therapeutic potentials. *Prog Neurobiol* 2014; 115: 138–156.
15. Zhang H, Prabhakar P, Sealock R et al. Wide genetic variation in the native pial collateral circulation is a major determinant of variation in severity of stroke. *J Cereb Blood Flow Metab* 2010; 30(5): 923–34.
16. Marchal G, Beaudouin V, Rioux P et al. Prolonged persistence of substantial volumes of potentially viable brain tissue after stroke: a correlative PET-CT study with voxel-based data analysis. *Stroke* 1996; 27: 599–606.
17. Copen WA, Rezai GL, Barak ER et al. Existence of the diffusion-blood flow mismatch within 24 hours after onset of acute stroke: dependence on proximal arterial occlusion. *Radiology* 2009; 250: 878–886.

18. Jovin TG, Yonas H, Gebel JM et al. The cortical ischemic core and not the consistently present penumbra is a determinant of clinical outcome in acute middle cerebral artery occlusion. *Stroke* 2003; 34(10): 2426-33.
19. Hakimelahi R, Vachha BA, Copen WA et al. Time and diffusion lesion size in major anterior circulation ischemic strokes. *Stroke* 2014; 45: 2936–2941.
20. Wheeler HM, Mlynash M, Inoue M et al. The growth rate of early DWI lesions is highly variable and associated with penumbral salvage and clinical outcomes following endovascular reblood flow. *Int J Stroke* 2015; 10: 723–729.
21. McCabe C, Gallagher L, Gsell W et al. Differences in the evolution of the ischemic penumbra in stroke-prone spontaneously hypertensive and Wistar-Kyoto rats. *Stroke* 2009; 40: 3864–3868.
22. Reid E, Graham D, Lopez-Gonzalez MR et al. Penumbra detection using PWI/DWI mismatch MRI in a rat stroke model with and without comorbidity: comparison of methods. *J. Cerebral Blood Flow Metab* 2012; 32: 1765–1777.
23. Tarr D, Graham D, Roy LA et al. Hyperglycemia accelerates apparent diffusion coefficient-defined lesion growth after focal cerebral ischemia in rats with and without features of metabolic syndrome. *J Cereb Blood Flow Metab* 2013; 33: 1556-63.
24. Boas DA, Dunn AK. Laser speckle contrast imaging in biomedical optics. *J Biomed Opt* 2010; 15(1): 011109.

25. Wang Z, Yang Y, Xiang X, Zhu Y, Men J and He M. Estimation of the normal range of blood glucose in rats. *Journal of Hygiene Research* 2010; 39(2): 133-142.
26. Koizumi JYY, Nakazawa T, Ooneda G. Experimental studies of ischemic brain edema. A new experimental model of cerebral embolism in rats in which recirculation can be introduced in the ischemic area. *Jpn J Stroke* 1986; 8: 1–8.
27. Tamura A, Graham DI, McCulloch J et al. Focal cerebral ischaemia in the rat: regional cerebral blood flow determined by [14c] Iodoantipyrine autoradiography following middle cerebral artery occlusion. *J Cereb Blood Flow Metab* 1981; 1: 61-9.
28. Shen Q, Meng X, Fisher M et al. Pixel-by-pixel spatiotemporal progression of focal ischemia derived using quantitative blood flow and diffusion imaging. *J Cereb Blood Flow Metab* 2003; 23: 1479-88.
29. Hossmann KA. Viability thresholds and the penumbra of focal ischemia. *Ann Neurol* 1994; 36: 557-65.
30. Bermudez E, Ferng S-F, Castro CE et al. DNA strand breaks caused by exposure to ozone and nitrogen dioxide. *Environmental Research* 1999; 81: 72–80.
31. Roustit M, Millet C, Blaise S et al. Excellent reproducibility of laser speckle contrast imaging to assess skin microvascular reactivity. *Microvasc Res* 2010; 80: 505–511.
32. Tew GA, Klonizakis M, Crank H et al. Comparison of laser speckle contrast imaging with laser doppler for assessing microvascular function. *Microvascular Research* 2011; 82: 326–332.

33. Briers JD. Laser speckle contrast imaging for measuring blood flow. *Optica Applicata* 2007; 36: 1–2.
34. Omarjee L, Signolet I, Humeau-Heutier A, Martin L, Henrion D, Pierre Abraham P. Optimisation of movement detection and artifact removal during laser speckle contrast imaging. *Microvascular Research* 2015; 97: 75-80.
35. Ayata C, Shin HK, Salomone S, Ozdemir-Gursoy Y, Boas DA, Dunn AK, Moskowitz MA. Pronounced hypoperfusion during spreading depression in mouse cortex. *J. Cereb. Blood Flow Metab* 2004; 24: 1172-1182.
36. Parthasarathy AB, Kazmi SMS, Dunn AK. Quantitative imaging of ischemic stroke through thinned skull in mice with Multi Exposure Speckle Imaging. *Biomedical Optics Express* 2010; 1(1): 258.
37. Liebeskind DS. Collateral blood flow: time for novel paradigms in cerebral ischemia. *Int J Stroke* 2012; 7: 309–310.
38. Strong AL, Anderson PJ, Watts HR et al. Peri-infarct depolarizations lead to loss of blood flow in ischaemic gyrencephalic cerebral cortex. *Brain* 2007; 130(4): 995–1008.
39. Armitage GA, Todd KG, Shuaib A et al. Laser speckle contrast imaging of cortical collateral blood flow during acute ischaemic stroke. *J Cereb Blood Flow Metab* 2010; 30: 1432–6.

40. Wang Z, Luo W, Zhou F et al. Dynamic change of collateral flow varying with distribution of regional blood flow in acute ischemic rat cortex. *J Biomed Opt* 2012; 17(12): 125001.
41. Qureshi AI, El-Gengaihi A, Hussein HM et al. Occurrence and variability in acute formation of leptomeningeal collaterals in proximal middle cerebral artery occlusion. *J Vasc Interv Neurol* 2008; 1: 70–72.
42. Liu W, Xu G, Yue X. Hyperintense vessels on flair: a useful non-invasive method for assessing intracerebral collaterals. *Eur J Radiol* 2011; 80: 786–791.
43. Fitch W, Edvinsson L, Watson R et al. Influences of pentobarbital and α -chloralose on cerebrovascular responses to vasoactive agents. *J Cereb Blood Flow Metab* 1983; 3(1): S520-S521.
44. Ueki M, Mies G, Hossmann KA. Effect of alpha-chloralose, halothane, pentobarbital and nitrous oxide anesthesia on metabolic coupling in somatosensory cortex of rat. *Acta Anaesthesiol Scand* 1992; 36: 318–322.
45. Dalkara T, Irikura K, Huang Z et al. Cerebrovascular responses under controlled and monitored physiological conditions in the anesthetized mouse. *J Cereb Blood Flow Metab* 1995; 15(4): 631–8.
46. Lewis NCS, Messinger L, Monteleone B et al. Effect of acute hypoxia on regional cerebral blood flow: effect of sympathetic nerve activity. *Journal of Applied Physiology* 2014; 116(9): 1189–96.

47. Bruno A, Biller J, Adams HP Jr et al. Acute blood glucose level and outcome from ischemic stroke: Trial of ORG 10172 in Acute Stroke Treatment (TOAST) Investigators. *Neurology* 1999; 52: 280–284.
48. Yao M, Ni J, Zhou L et al. Elevated Fasting Blood Glucose Is Predictive of Poor Outcome in Non-Diabetic Stroke Patients: A Sub-Group Analysis of SMART. *PLoS One* 2016; 11(8): e0160674.
49. Kiers L, Davis SM, Larkins R et al. Stroke topography and outcome in relation to hyperglycaemia and diabetes. *J Neurol Neurosurg Psychiatry* 1992; 55: 263-70.
50. Tuttolomondo A, Pinto A, Salemi G et al. Diabetic and non-diabetic subjects with ischemic stroke: Differences, subtype distribution and outcome. *Nutr Metab Cardiovasc Dis* 2008; 18(2): 152-7.
51. Ntaios G, Egli M, Faouzi M et al. J-shaped association between serum glucose and functional outcome in acute ischemic stroke. *Stroke* 2010; 41: 2366–70.
52. Shimoyama T, Kimura K, Uemura J et al. Elevated glucose level adversely affects infarct volume growth and neurological deterioration in non-diabetic stroke patients, but not diabetic stroke patients. *Eur J Neurol* 2014; 21: 402-10.
53. Mi D, Wang P, Yang B et al. Correlation of hyperglycemia with mortality after acute ischemic stroke. *Ther Adv Neurol Disord* 2018; 11: 1–5.
54. Menon BK, Smith EE, Coutts SB et al. Leptomeningeal collaterals are associated with modifiable metabolic risk factors. *Ann. Neurol* 2013; 74(2): 241-8.

55. Kim JT, Liebeskind DS, Jahan R, Menon BK, Goyal M, Nogueira RG, Pereira VM, Gralla J, Saver JL. Impact of Hyperglycemia According to the Collateral Status on Outcomes in Mechanical Thrombectomy. *Stroke* 2018; 49(11):2706-2714.
56. Thow LA, MacDonald K, Holmes WM et al. Hyperglycaemia does not increase perfusion deficits after focal cerebral ischaemia in male Wistar rats. *Brain and Neuroscience Advances* 2018; 2: 1-13.
57. Mayhan WG, Patel KP. Acute effects of glucose on reactivity of cerebral microcirculation: role of activation of protein kinase c. *Am J Physiol* 1995; 269: H1297-302.
58. Du XL, Edelstein D, Dimmeler S et al. Hyperglycaemia inhibits endothelial nitric oxide synthase activity by posttranslational modification at the AKT site. *J Clin Invest* 2001; 108(9): 1341–1348.
59. Lemkes BA, Hermanides J, Devries JH et al. Hyperglycemia: a prothrombotic factor? *J Thromb Haemost* 2010; 8: 1663-9.
60. Leonardi-Bee J, Bath PM, Phillips SJ et al. 1ST Collaborative Group. Blood pressure and clinical outcomes in the International Stroke Trial. *Stroke* 2002; 33: 1315–1320.
61. Okumura K, Ohya Y, Maehara A et al. Effects of blood pressure levels on case fatality after acute stroke. *J Hypertens* 2005; 23: 1217–1223.
62. Yamori Y, Horie R, Handa H et al. Pathogenetic similarity of strokes in stroke-prone spontaneously hypertensive rats and humans. *Stroke* 1976; 7: 46–53.

63. Okamoto K, Yamori Y, Nagaoka A. Establishment of the stroke-prone spontaneously hypertensive rat (SHR). *Circ Res* 1974; 34/35(1): 143–153.
64. Chan SL, Bishop N, Li Z and Cipolla MJ. Inhibition of PAI (Plasminogen Activator Inhibitor)-1 Improves Brain Collateral Perfusion and Injury After Acute Ischemic Stroke in Aged Hypertensive Rats. *Stroke* 2018; 49(8): 1969-1976.
65. Cipolla MJ, Linfante I, Abuchowski A, Jubin R, Chan S-L. Pharmacologically increasing collateral perfusion during acute stroke using a carboxyhemoglobin gas transfer agent (Sanguinate™) in spontaneously hypertensive rats. *J. Cereb. Blood Flow and Metab.* 2018; 38(5): 755–766.
66. Coyle P, Heistad DD. Development of collaterals in the cerebral circulation. *Blood Vessels* 1991; 28(1-3): 183-189.
67. Jeffs B, Clark J, Anderson N et al. Sensitivity to cerebral ischaemic insult in a rat model of stroke is determined by a single genetic locus. *Nature Genet* 1997; 16: 364–367.
68. Carswell HV, Anderson NH, Clark JS et al. Genetic and gender influences on sensitivity to focal cerebral ischemia in the stroke-prone spontaneously hypertensive rat. *Hypertension* 1999; 33: 681-5.
69. McGill JK, Gallagher L, Carswell HVO et al. Impaired functional recovery after stroke in the stroke-prone spontaneously hypertensive rat. *Stroke* 2005; 36: 135–141.

70. Gemba T, Matsunaga K, Ueda M. Changes in extracellular concentration of amino acids in the hippocampus during cerebral ischemia in stroke-prone SHR, stroke-resistant SHR and normotensive rats. *Neurosci Lett* 1992; 135: 184-8.
71. Dunn KM, Renic M, Flasch AK et al. Elevated production of 20-HETE in the cerebral vasculature contributes to severity of ischemic stroke and oxidative stress in spontaneously hypertensive rats. *Am J Physiol Heart Circ Physiol* 2008; 295: 2455-65.
72. Terpolilli NA, Kim SW, Thal SC et al. Inhalation of nitric oxide prevents ischemic brain damage in experimental stroke by selective dilatation of collateral arterioles. *Circ Res* 2012; 110(5): 727-38.
73. Chan SL, Sweet JG, Bishop N and Cipolla MJ. Pial collateral reactivity during hypertension and aging. *Stroke* 2016. 47(6): 1618–1625.
74. Chan SL, Bishop N, Li Z, Cipolla MJ. Inhibition of PAI (Plasminogen Activator Inhibitor)-1 Improves Brain Collateral Perfusion and Injury After Acute Ischemic Stroke in Aged Hypertensive Rats. *Stroke* 2018; 49(8):1969-1976.
75. Kazmi SMS, Parthasarthy AB, Song NE, Jones TA, Dunn AK. Chronic imaging of cortical blood flow using Multi-Exposure Speckle Imaging. *J. Cereb. Blood Flow and Metab* 2013; 33: 798–808.
76. Ma J, Ma Y, Dong B, Bandet MV, Shuaib A, Winship IR. Prevention of the collapse of pial collaterals by remote ischemic preconditioning during acute ischemic stroke. *J. Cereb. Blood Flow and Metab.* 2017; 37(8): 3001–3014.

77. Winship IR, Armitage GA, Ramakrishnan G, Dong B, Todd KG, Shuaib A (2014).
Augmenting collateral blood flow during ischemic stroke via transient aortic occlusion.
J. Cereb. Blood Flow and Metab. 2014; 34: 61–71.

FIGURE LEGENDS

Figure 1. Laser speckle contrast imaging set up and analysis. (A) A representative laser speckle image showing normally perfused rat brain with superior cortical vessels before pMCAO was induced. (B) A representative laser speckle image of the cortical surface following pMCAO, showing normal blood flow in the contralateral hemisphere (red-yellow) and cortical blood flow deficit in the ipsilateral hemisphere (blue-black). (C) Regions of interest (ROIs) on the LSCI defined with applied CBF thresholds: ischaemic core (cortical blood flow <43% of mean contralateral hemisphere), hypoperfused tissue (cortical blood flow between 43-75% of mean contralateral hemisphere) along with contralateral equivalent ROIs.

Figure 2. Recruitment of cortical collateral blood flow post-MCAO. (A) Cortical blood flow map of a representative rat per group. (B) Increase in cortical blood flow in the ROIs of the ipsilateral hemisphere following pMCAO while blood flow remained relatively unchanged in the non-stroke control group over time. Cortical blood flow values for each ROI were normalised to their respective 10min average at baseline and the entire ipsilateral hemisphere was the ROI for non-stroke controls. (C) Area under curve of cortical perfusion in the ipsilateral hemisphere ROIs used to test the statistical difference between groups over the time course of ischaemia (0.5-4h) and analysed using Student's unpaired t-test, $p > 0.05^*$. (D) Cortical blood flow was unchanged from

baseline in all equivalent ROIs in the contralateral hemisphere. (E) Area under curve for cortical perfusion in the contralateral hemisphere ROIs, over the time course of ischaemia. (F) No significant change in MABP over the time course of the experiment. Area under curve data for cortical perfusion presented as mean \pm SD, other data presented as mean + SD.

Figure 3. Impact of acute hyperglycaemia on cortical collateral blood flow. (A) Cortical blood flow map of a representative rat per group. (B) Cortical blood flow in the ipsilateral ischaemic core ROI. (C) Area under curve for cortical perfusion (0.5-4h) in the ipsilateral ischaemic core ROI of vehicle and glucose groups, $p>0.05^*$. (D) Cortical blood flow in the ipsilateral hypoperfused ROI. (E). Area under curve of cortical perfusion (0.5-4h) in the ipsilateral hypoperfused ROI. (F) Cortical perfusion in the ROI contralateral to ischaemic core. (G) Area under curve of cortical perfusion in the ROI contralateral to ischaemic core, $p>0.05^*$. (H) Cortical perfusion in the ROI contralateral to the hypoperfused ROI. (I) Area under curve of cortical perfusion in the ROI contralateral to the hypoperfused ROI, $p>0.05^*$. (J) MABP, stable over the time course of ischaemia, in vehicle and glucose groups. (K) Blood glucose concentration 10min prior to and during the time course of ischaemia. Analysed using repeated measures 2way ANOVA, $p=0.0001^*$. Area under curve data for cortical perfusion presented as mean \pm SD, other data presented as mean + SD.

Figure 4. Impact of chronic hypertension on cortical collateral blood flow. (A) Cortical blood flow map of a representative SHRSP rat following pMCAO. (B) Cortical blood flow normalised to the respective 10min average at baseline in the ipsilateral ischaemic core and equivalent contralateral ROI. (C) Area under curve of cortical perfusion in the ipsilateral ischaemic core and equivalent contralateral ROI, over the time course of ischaemia (0.5-4h), analysed using Student's unpaired t-test, $p > 0.05^*$. (D) Cortical blood flow, normalised to the respective 10min average at baseline, in hypoperfused ROI and equivalent contralateral ROI. (E) Area under curve of cortical perfusion for hypoperfused ROI and equivalent contralateral ROI. (F) MABP data over the time course of ischaemia. Area under curve data for cortical perfusion presented as mean \pm SD, other data presented as mean + SD.

Figure 5. Influence of iNO on cortical collateral recruitment post-MCAO. (A) Cortical blood flow map for representative rat per group over the time course of ischaemia. (B) Cortical blood flow, normalised to the respective 10min average at baseline, in the ipsilateral ischaemic core ROI. (C) Area under curve of cortical perfusion in the ipsilateral ischaemic core ROI over the time course of ischaemia (0.5-4h). (D) Cortical blood flow, normalised to the respective 10min average at baseline, in the ipsilateral hypoperfused ROI. (E) Area under curve for cortical perfusion in the ipsilateral hypoperfused ROI. (F) Cortical perfusion, normalised to the respective

10min average at baseline, in the ROI contralateral to ischaemic core. (G) Area under curve of cortical perfusion for ROI contralateral to ischaemic core. (H) Cortical perfusion, normalised to the respective 10min average at baseline, in the ROI contralateral to hypoperfused ROI. (I) Area under curve of cortical perfusion for ROI contralateral to hypoperfused ROI. (J) MABP over the time course of ischaemia in Air and iNO groups. (K) Blood glucose concentration 10min prior to and during the time course of ischaemia. Area under curve data for cortical perfusion presented as mean \pm SD, other data presented as mean + SD.

FIGURES AND FIGURE LEGENDS

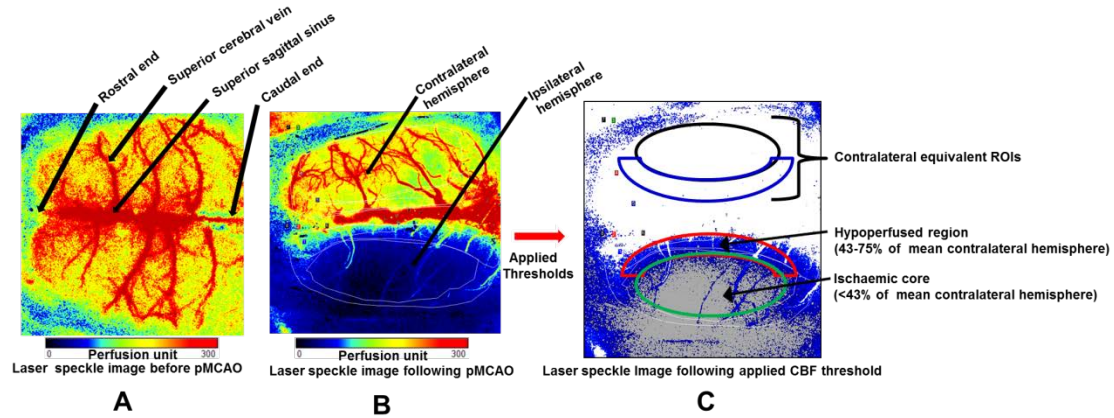


Figure 1. Laser speckle contrast imaging set up and analysis. (A) A representative laser speckle image showing normally perfused rat brain with superior cortical vessels before pMCAO was induced. (B) A representative laser speckle image of the cortical surface following pMCAO, showing normal blood flow in the contralateral hemisphere (red-yellow) and cortical blood flow deficit in the ipsilateral hemisphere (blue-black). (C) Regions of interest (ROIs) on the LSCI defined with applied CBF thresholds: ischaemic core (cortical blood flow <43% of mean contralateral hemisphere), hypoperfused tissue (cortical blood flow between 43-75% of mean contralateral hemisphere) along with contralateral equivalent ROIs.

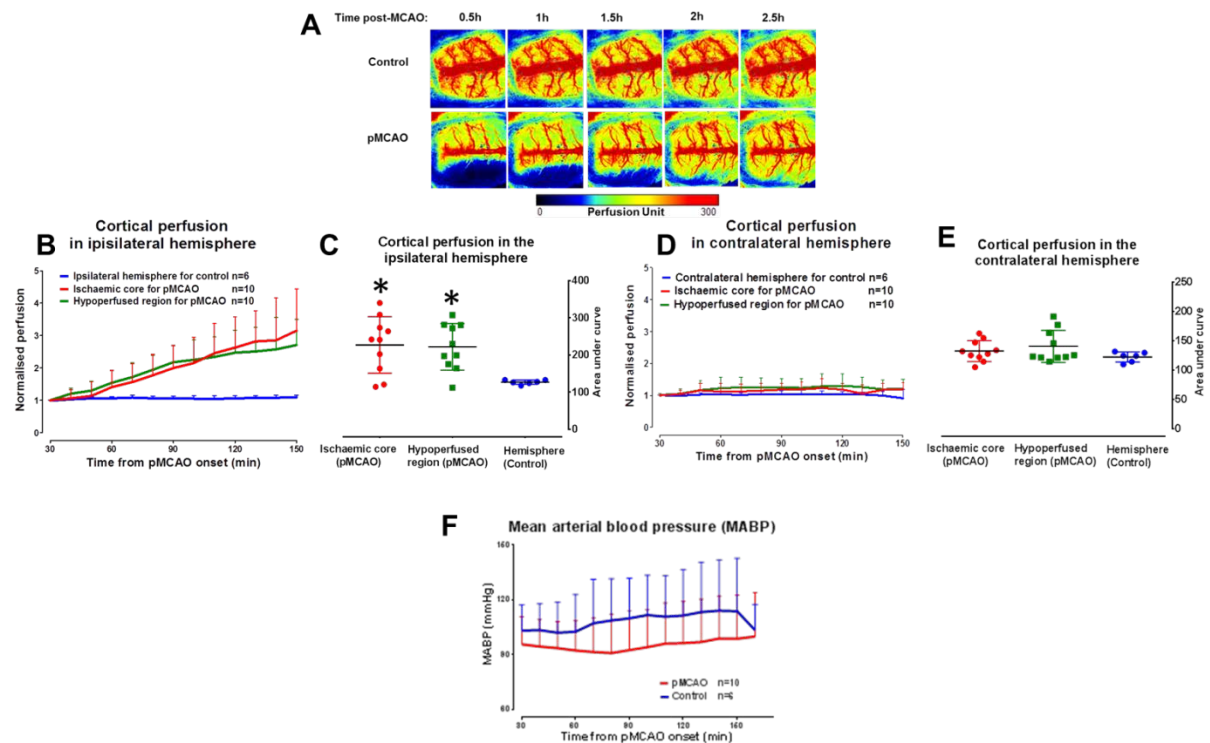


Figure 2. Recruitment of cortical collateral blood flow post-MCAO. (A) Cortical blood flow map of a representative rat per group. (B) Increase in cortical blood flow in the ROIs of the ipsilateral hemisphere following pMCAO while blood flow remained relatively unchanged in the non-stroke control group over time. Cortical blood flow values for each ROI were normalised to their respective 10min average at baseline and the entire ipsilateral hemisphere was the ROI for non-stroke controls. (C) Area under curve of cortical perfusion in the ipsilateral hemisphere ROIs used to test the statistical difference between groups over the time course of ischaemia (0.5-4h) and analysed using Student's unpaired t-test, $p > 0.05^*$. (D) Cortical blood flow was unchanged from baseline in all equivalent ROIs in the contralateral hemisphere. (E) Area under curve for cortical perfusion in the contralateral hemisphere ROIs, over the time course of ischaemia. (F) No significant change in MABP over the time course of the experiment. Area under curve data for cortical perfusion presented as mean \pm SD, other data presented as mean + SD.

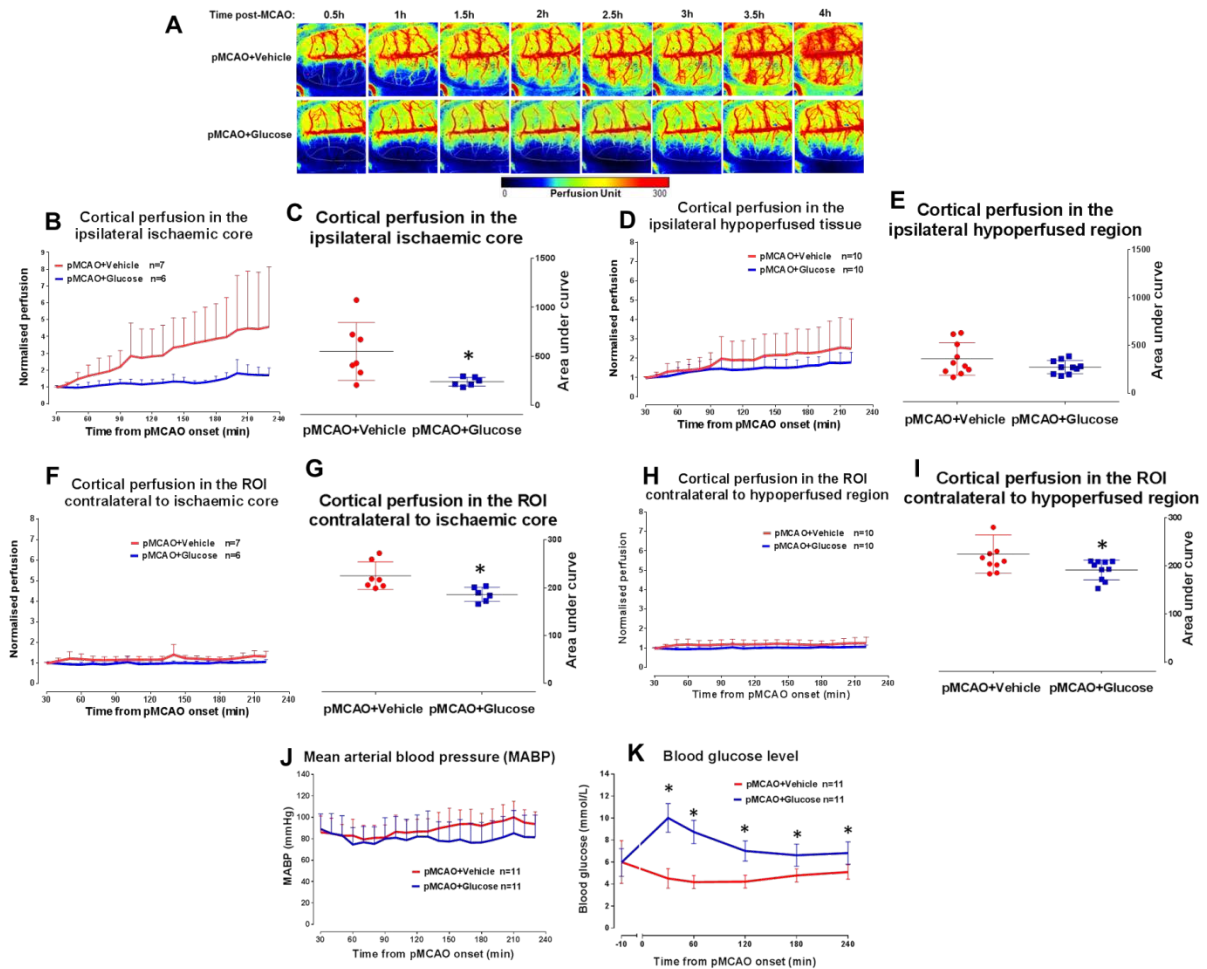


Figure 3. Impact of acute hyperglycaemia on cortical collateral blood flow. (A) Cortical blood flow map of a representative rat per group. (B) Cortical blood flow in the ipsilateral ischaemic core ROI. (C) Area under curve for cortical perfusion (0.5-4h) in the ipsilateral ischaemic core ROI of vehicle and glucose groups, $p > 0.05^*$. (D) Cortical blood flow in the ipsilateral hypoperfused ROI. (E). Area under curve of cortical perfusion (0.5-4h) in the ipsilateral hypoperfused ROI. (F) Cortical perfusion in the ROI contralateral to ischaemic core. (G) Area under curve of cortical perfusion in the ROI contralateral to ischaemic core, $p > 0.05^*$. (H) Cortical perfusion in the ROI contralateral to the hypoperfused ROI. (I) Area under curve of cortical perfusion in the ROI contralateral to the hypoperfused ROI, $p > 0.05^*$. (J) MABP, stable over the time course of ischaemia, in vehicle and glucose groups. (K) Blood glucose concentration 10min prior to and during the time course of ischaemia. Analysed using repeated measures 2way ANOVA, $p = 0.0001^*$. Area under curve data for cortical perfusion presented as mean \pm SD, other data presented as mean + SD.

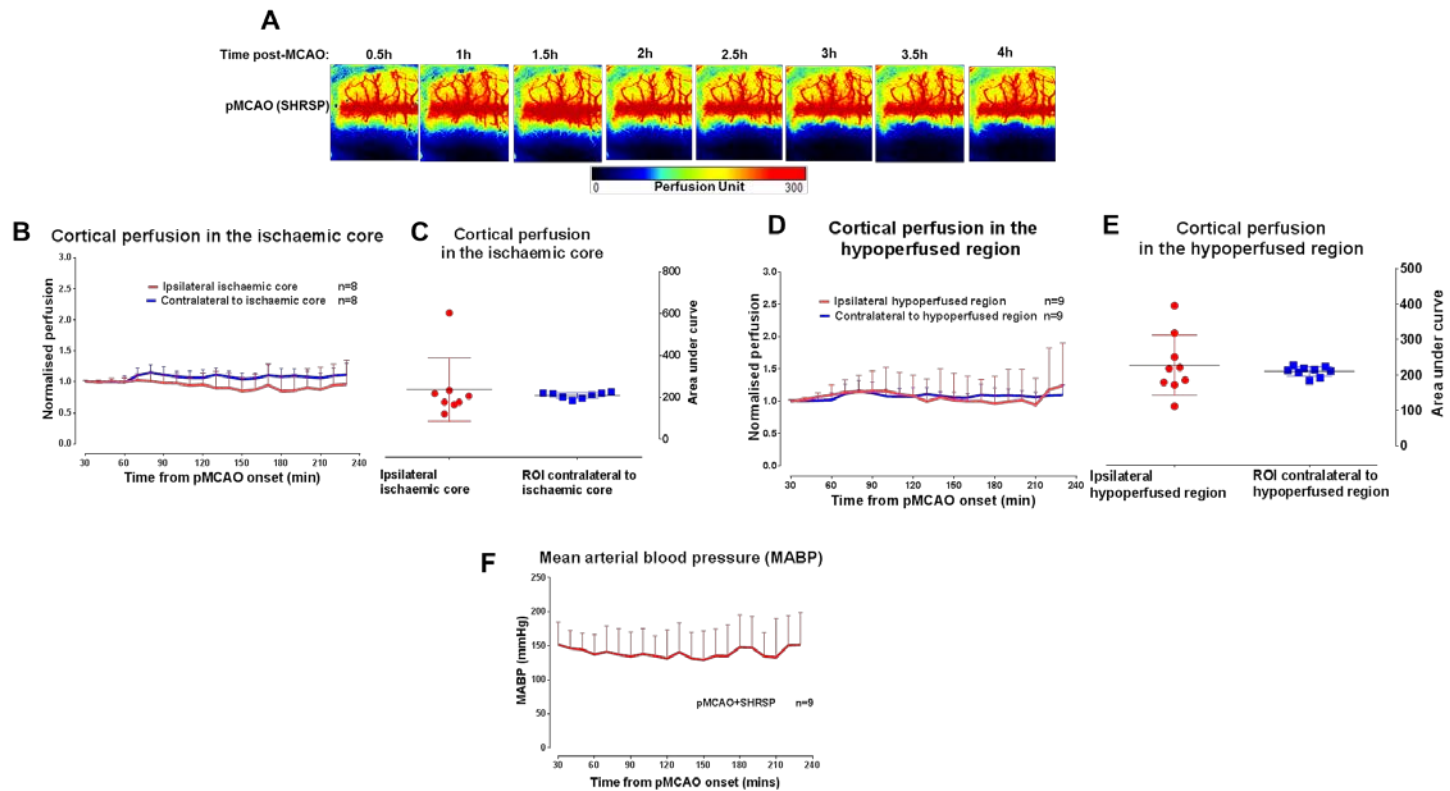


Figure 4. Impact of chronic hypertension on cortical collateral blood flow. (A) Cortical blood flow map of a representative SHRSP rat following pMCAO. (B) Cortical blood flow normalised to the respective 10min average at baseline in the ipsilateral ischaemic core and equivalent contralateral ROI. (C) Area under curve of cortical perfusion in the ipsilateral ischaemic core and equivalent contralateral ROI, over the time course of ischaemia (0.5-4h), analysed using Student's unpaired t-test, $p > 0.05^*$. (D) Cortical blood flow, normalised to the respective 10min average at baseline, in hypoperfused ROI and equivalent contralateral ROI. (E) Area under curve of cortical perfusion for hypoperfused ROI and equivalent contralateral ROI. (F) MABP data over the time course of ischaemia. Area under curve data for cortical perfusion presented as mean \pm SD, other data presented as mean + SD.

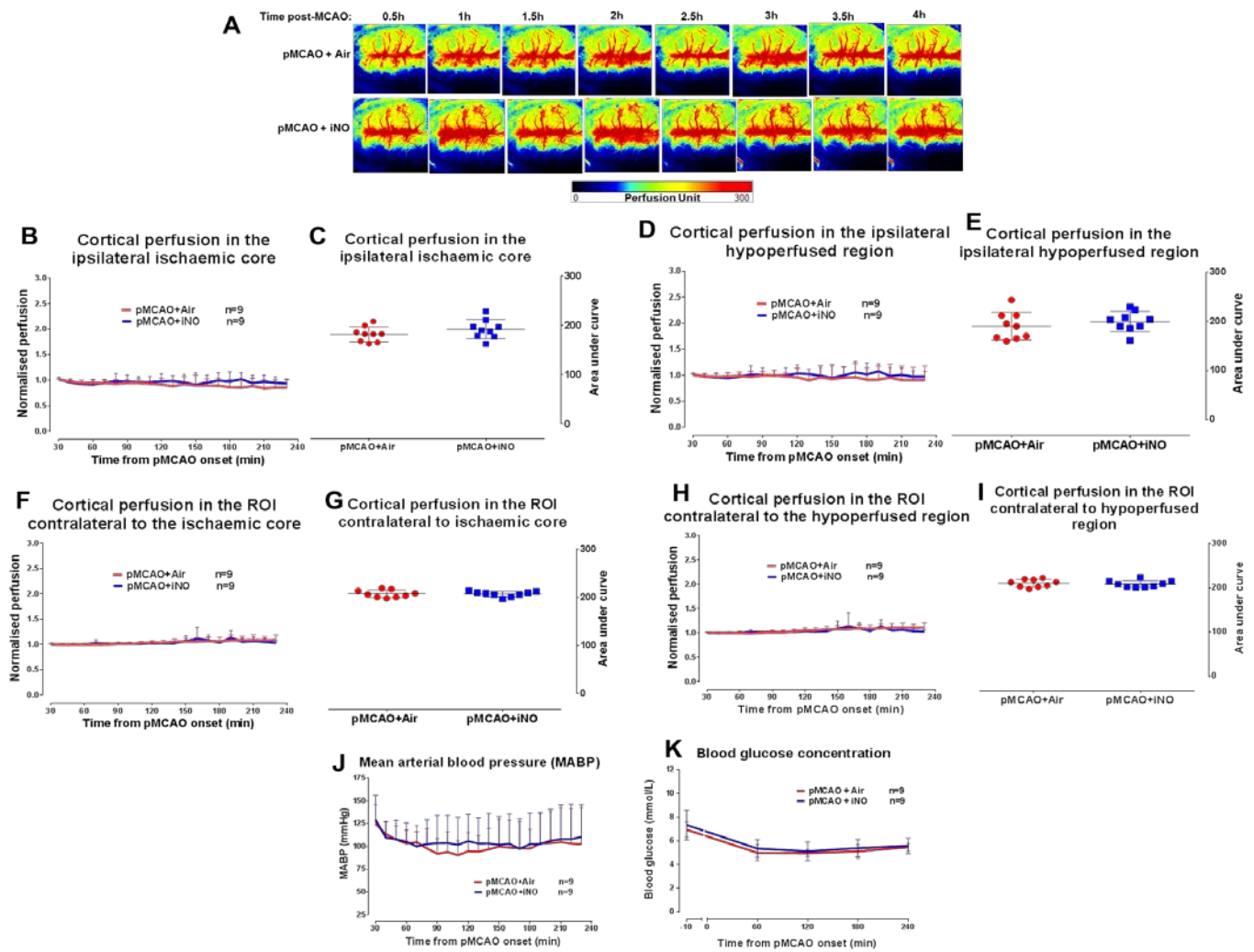


Figure 5. Influence of iNO on cortical collateral recruitment post-MCAO. (A) Cortical blood flow map for representative rat per group over the time course of ischaemia. (B) Cortical blood flow, normalised to the respective 10min average at baseline, in the ipsilateral ischaemic core ROI. (C) Area under curve of cortical perfusion in the ipsilateral ischaemic core ROI over the time course of ischaemia (0.5-4h). (D) Cortical blood flow, normalised to the respective 10min average at baseline, in the ipsilateral hypoperfused ROI. (E) Area under curve for cortical perfusion in the ipsilateral hypoperfused ROI. (F) Cortical perfusion, normalised to the respective 10min average at baseline, in the ROI contralateral to ischaemic core. (G) Area under curve of cortical perfusion for ROI contralateral to ischaemic core. (H) Cortical perfusion, normalised to the respective 10min average at baseline, in the ROI contralateral to hypoperfused ROI. (I) Area under curve of cortical perfusion for ROI contralateral to hypoperfused ROI. (J) MABP over the time course of ischaemia in Air and iNO groups. (K) Blood glucose concentration 10min prior to and during the time course of ischaemia. Area under curve data for cortical perfusion presented as mean \pm SD, other data presented as mean + SD.